THE JOURNAL OF BIOLOGICAL CHEMISTRY VOL. 281, NO. 7, pp. 4164–4172, February 17, 2006

Beads-on-a-String, Characterization of Ets-1 Sumoylated within Its Flexible N-terminal Sequence*[S]

Received for publication, September 26, 2005, and in revised form, November 28, 2005 Published, JBC Papers in Press, November 29, 2005, DOI 10.1074/jbc.M510488200

Matthew S. Macauley[‡1], Wesley J. Errington[‡1], Manuela Schärpf[‡], Cameron D. Mackereth[‡], Adam G. Blaszczak[§], Barbara J. Graves[§2], and Lawrence P. McIntosh[‡3]

From the [‡]Department of Biochemistry and Molecular Biology, Department of Chemistry, and The Michael Smith Laboratories, University of British Columbia, Vancouver, British Columbia, V6T 1Z3, Canada and the [§]Department of Oncological Sciences, Huntsman Cancer Institute, University of Utah, Salt Lake City, Utah 84112

Sumoylation regulates the activities of several members of the ETS transcription factor family. To provide a molecular framework for understanding this regulation, we have characterized the conjugation of Ets-1 with SUMO-1. Ets-1 is modified *in vivo* predominantly at a consensus sumoylation motif containing Lys-15. This lysine is located within the unstructured N-terminal segment of Ets-1 preceding its PNT domain. Using NMR spectroscopy, we demonstrate that the Ets-1 sumoylation motif associates with the substrate binding site on the SUMO-conjugating enzyme UBC9 (K_d ~400 μM) and that the PNT domain is not involved in this interaction. Ets-1 with Lys-15 mutated to an arginine still binds UBC9 with an affinity similar to the wild type protein, but is no longer sumoylated. NMR chemical shift and relaxation measurements reveal that the covalent attachment of mature SUMO-1, via its flexible C-terminal Gly-97, to Lys-15 of Ets-1 does not perturb the structure or dynamic properties of either protein. Therefore sumoylated Ets-1 behaves as "beads-on-a-string" with the two proteins tethered by flexible polypeptide segments containing the isopeptide linkage. Accordingly, SUMO-1 may mediate interactions of Ets-1 with signaling or transcriptional regulatory macromolecules by acting as a structurally independent docking module, rather than through the induction of a conformational change in either protein upon their covalent linkage. We also hypothesize that the flexibility of the linking polypeptide sequence may be a general feature contributing to the recognition of SUMO-modified proteins by their downstream effectors.

The regulation of gene expression requires the spatial and temporal orchestration of a complex network of protein-protein and protein-DNA interactions. Central to the control of these interactions are a myriad of post-translational modifications. One such modification involves the reversible, covalent attachment of the ubiquitin-like protein SUMO.[4] In addition to serving as an antagonist against ubiquitin-mediated degradation, sumoylation affects a growing number of recognized biological processes, including nuclear transport, signal transduction, transcription, and DNA repair (recent reviews Refs. 1–5). However, despite extensive studies, the molecular mechanisms for this regulation, which likely arise through SUMO-dependent modulation of target protein interactions with other macromolecules, remain largely undefined (2, 6–8).

In contrast, the pathways for the sumoylation and desumoylation of target proteins are well established. After proteolytic maturation and ATP-dependent activation, SUMO family members are transferred from the heterodimeric E1-activating enzyme to Cys-93 in the single E2-conjugating enzyme, UBC9. Although E3-ligating enzymes, which facilitate the specificity and efficiency of sumoylation, have been identified, UBC9 is sufficient for conjugating SUMO to many proteins, at least *in vitro* (9). The final product is an isopeptide bond joining the C-terminal glycine carboxyl of SUMO with the side chain amino group of a lysine in the target protein. This lysine is generally present in a ψ*KX*E/D consensus motif, where ψ represents a large branched hydrophobic residue (Ile, Val, or Leu) and *X* is any amino acid (10, 11). The molecular determinants for the recognition of this motif were revealed by the crystal structure of the C-terminal domain of RanGAP1 bound to UBC9 (6, 12). Completing the pathway, desumoylation of modified proteins results from proteolytic cleavage of the isopeptide bond by SUMO-specific proteases (13, 14).

As revealed by recent proteome-wide analyses, transcription is one of the most prevalent processes associated with sumoylation (9, 15–17). Transcription factors, as well as co-activators and co-repressors, are frequently SUMO targets, and in most cases, their sumoylation leads to transcriptional repression (recent reviews Refs. 18–20). The regulation of transcription factors by SUMO conjugation arises through several possible mechanisms. Sumoylation may compete with alternative post-translational modifications, such as ubiquitinylation, acetylation, or methylation, of key lysine residues in transcription factors. Sumoylation can also alter the cellular localization or stability of a protein involved in signal transduction or transcription, as seen with Smad4, TEL, and Elk-1 (21–23). More specifically, sumoylation is often involved in modulating the subnuclear distribution of transcription factors. Conjugation of the promyelocytic leukemia protein with SUMO leads to the formation of nuclear subdomains, variously termed nuclear bodies, promyelocytic

* This research was supported in part by grants from National Cancer Institute of Canada with funds from the Canadian Cancer Society (to L. P. M.) and the National Institutes of Health Grants GM38663 (to B. J. G.) and CA24014 (to the Huntsman Cancer Institute). Instrument support was provided by the Protein Engineering Network of Centres of Excellence, the Canadian Foundation for Innovation, the British Columbia Knowledge Development Fund, the UBC Blusson Fund, and the Michael Smith Foundation for Health Research. The costs of publication of this article were defrayed in part by the payment of page charges. This article must therefore be hereby marked "*advertisement*" in accordance with 18 U.S.C. Section 1734 solely to indicate this fact.

[S] The on-line version of this article (available at http://www.jbc.org) contains supplemental Figs. S1–S5.

[1] Both authors contributed equally to this work.

[2] Received funding from the United States Department of Energy and the Huntsman Cancer Foundation.

[3] A Canadian Institute for Health Research Scientist. To whom correspondence should be addressed: Dept. of Biochemistry and Molecular Biology, 2350 Health Sciences Mall, University of British Columbia. Vancouver, B.C., Canada, V6T 1Z3. Tel.: 604-822-3341; Fax: 604-822-5227; E-mail: mcintosh@chem.ubc.ca.

[4] The abbreviations used are: SUMO, small ubiquitin-like modifier; E1, ubiquitin-like protein- activating enzyme; E2, ubiquitin-like protein-conjugating enzyme; E3, ubiquitin-like protein- isopeptide ligase; GST, glutathione *S*-transferase; HA, hemagglutinin; HSQC, heteronuclear single quantum correlation; NOE, nuclear Overhauser effect; SUMO-1_{gg}, residues 1–97 of human SUMO-1 plus an N-terminal Gly-Ser-His tripeptide; TOCSY, total correlation spectroscopy; NOESY, nuclear Overhauser effect spectroscopy.

leukemia protein bodies, or PODs (promyelocytic leukemia protein oncogenic domains), to which additional transcription factors, such as Sp100, LEF-1, and p53, associate. Nuclear bodies may serve as storage sites for regulatory factors or may function in specific activities such as the modification or assembly of transcription complexes (24, 25). Alternatively, sumoylated transcription factors can recruit co-repressors, such as histone deactylases or Daxx, to promoters and thereby induce possible changes in chromatin structure leading to reduced gene expression (26–28). Although generally associated with repression, sumoylation can also result in enhanced transcriptional activation, as seen with the heat shock factors HSF1 and HSF2 (29). Adding further complexity, sumoylation of transcription factors may be reinforced or opposed by additional regulatory modifications, such as phosphorylation (30, 31).

Several members of the ETS transcription factor family are regulated by sumoylation. Initial clues for this regulation came through approaches, such as yeast two-hybrid screens, identifying UBC9 as an interacting partner with ETS family members including Ets-1 (32), TEL (33), LIN-1 (34), Net (35), and ERM (36). Modification of TEL with SUMO-1 reduces its activity as a transcriptional repressor, possibly by causing targeting to nuclear speckles and/or enhanced export from the nucleus (23, 37). Sumoylation appears to occur predominantly at a non-consensus lysine residue within the PNT domain of TEL and to be abrogated by mutations that disrupt the self-association of this domain (23, 37). In contrast to TEL, sumoylation of other ETS family members studied to date results in reduced transcription. For example, addition of SUMO-1 to the R motif of Elk-1 promotes association with histone deacetylase HDAC-2, thereby leading to transcriptional repression (27). This dynamic regulatory pathway is opposed by the MAP kinase-dependent phosphorylation of Elk-1, which both increases the activity of its transactivation domain and causes the loss of SUMO-1 conjugation (30). Similarly, sumoylation of *Caenorhabditis elegans* LIN-1 appears to result in transcriptional repression of genes responsible for vulval cell fate by promoting binding to MEP-1, a protein associated with the NuRD nucleosome remodeling and histone deacetylation complex (34).

In this report, we have investigated the sumoylation of the ETS protein Ets-1 with a focus on characterizing its interactions with the conjugating enzyme UBC9 and on determining the structural and dynamic consequences of this modification. All vertebrate Ets-1 proteins display four conserved consensus sites for sumoylation (see Fig. 1*A*). Of these, we have characterized sumoylation at Lys-15 *in vivo* and *in vitro* within the context of a previously studied 15.5-kDa deletion fragment,[5] Ets-$1^{(1-138)}$, that is amenable to NMR spectroscopic analysis (38). By monitoring NMR spectral changes, we confirmed that Ets-$1^{(1-138)}$ binds the active site of UBC9 via the consensus sumoylation motif encompassing Lys-15. Furthermore, covalent attachment of SUMO-1 to Ets-$1^{(1-138)}$ does not perturb the structure or dynamic properties of either protein, indicating that they behave as "beads-on-a-string" tethered by a flexible isopeptide linkage. This site of sumoylation lies near a mitogen-activated protein kinase ERK2 phosphoacceptor site Thr-38 and the structured PNT domain of Ets-1 (residues 54–134). The PNT domain both serves as an ERK2 docking site (39) and, along with phosphorylated Thr-38, mediates recruitment of the CBP/p300 transcriptional co-activator (40). Thus, the sumoylation of Lys-15 may have biological consequences related to the functions of the N-terminal region of Ets-1.

[5] Ets-1 fragments are indicated by residues spanned; e.g. Ets-$1^{(1-138)}$ corresponds to residues 1–138 of the 440 amino acid protein.

EXPERIMENTAL PROCEDURES

DNA Constructs—Escherichia coli expression plasmids for murine His_6-FLAG-HMK-tagged Ets-$1^{(1-440)}$, His_6-tagged Ets-$1^{(1-138)}$, Ets-$1^{(51-138)}$, His_6- and GST-tagged mature human SUMO-1_{gg}, His_6- and GST-tagged human UBC9, His_6-tagged human E1 (SAE1/SAE2), and GST-tagged yeast E1 (Aos1/Uba2) have been described previously or were constructed as described previously (38, 39, 41–43). The gene encoding His_6-tagged Ets-$1^{(1-52)}$ was PCR-cloned into the pET28a vector (Novagen) with the substitution of Leu-49 to Trp to allow quantitation by UV light absorption spectrophotometry. Additional point mutations were introduced using the QuikChange method (Stratagene).

Mammalian Expression Vectors—CMV vector expressing FLAG-tagged full-length mouse Ets-1 was previously described (39). The K15R mutant was made with a QuikChange mutagenesis kit (Stratagene). Vectors encoding GAL4:Ets-$1^{(1-138)}$ and GAL4:Ets-$1^{(1-52)}$ were created from a GAL4 vector, pFA-CMV (40). The expression vector for HA-SUMO-1 has been described (44) and was a kind gift of Grace Gill, Harvard Medical School.

Protein Expression and Purification—Proteins were expressed using *E. coli* BL21 (λDE3) cells grown in LB medium or in M9 medium containing 1 g/liter $^{15}NH_4Cl$ and/or 3 g/liter $^{13}C_6$-glucose (Spectral Stable Isotopes). His_6- and GST-tagged proteins were purified using Ni^{2+}-(HisTrap, Amersham Biosciences) or glutathione-affinity (GSTrap) chromatography, respectively (43). Non-tagged Ets-$1^{(51-138)}$ was isolated by anion exchange chromatography (38, 39). The appropriate column fractions were pooled, dialyzed overnight into 10 mM NaCl, 50 mM Tris-Cl, 2 mM β-mercaptoethanol, pH 6.5 or 7.5, and concentrated by ultrafiltration. When necessary to cleave the His_6-tag, thrombin was included during the dialysis step and subsequently inactivated with *p*-aminobenzamidine beads (Sigma). Talon metal affinity resin (Clontech) was added in a batch method to remove the cleaved His_6-tag and any uncleaved protein. The resulting constructs contained an N-terminal Gly-Ser-His extension after proteolytic processing. The final sample concentrations were determined by UV spectrophotometry using predicted molar absorptivities (45). Electrospray ionization mass spectrometry and SDS-PAGE were used to confirm the mass and purity of each protein.

Antibodies—Rabbit anti-Ets-1 has been described (46). Rabbit anti-HA (Y-11) and anti-GAL4 were from Santa Cruz Biotechnology. Secondary antibody-horseradish-peroxidase conjugates were from Amersham Biosciences.

Immunoprecipitation of FLAG and GAL4-tagged Ets-1 Proteins—Approximately 1.5×10^6 NIH3T3 mouse fibroblasts were plated in 100-mm dishes and transfected the next day with 5 μg of FLAG-Ets-1 or GAL4-Ets-1 expression plasmid (or empty vector), 5 μg of mature HA-SUMO-1 (or empty vector), and 50 μl of Lipofectamine (Invitrogen). After transfection, cells were serum-starved as described (40). Cells were washed once with ice-cold phosphate-buffered saline and then scraped off dishes in 1 ml of RIPA buffer (50 mM Tris-Cl, pH 7.5, 150 mM NaCl, 1 mM EDTA, 1% Nonidet P-40, 1% sodium deoxycholate, 0.1% SDS, 1× complete miniprotease inhibitors (Roche Applied Science), and 1 mM phenylmethylsulfonyl fluoride) supplemented with 25 mM *N*-ethylmaleimide (Sigma). Cells were sonicated as described (40) and clarified at 20,900 × *g* for 15 min at 4 °C. Lysates were precleared with 40 μl of a 50% slurry of protein A-agarose (Pierce) at 4 °C for at least 30 min. To the cleared lysates, 40 μl of a 50% slurry of anti-FLAG M2 (Sigma) or anti-GAL4 affinity gel (Santa Cruz Biotechnology) was added, and incubation was continued at 4 °C for 1 h. Following three washes in RIPA buffer, 3× SDS-sample buffer was added to the beads, and eluted proteins were analyzed by 4–15% gradient SDS-PAGE and Western blot-

ting using antibodies against Ets-1, GAL4, or the HA epitope tag, as indicated in the figures.

In Vitro Sumoylation—Sumoylation reactions were carried out overnight at 37 °C using 50-μl or 50–100-ml solutions containing ~50 μM target protein, 50 μM SUMO-1_{gg}, 10 μM GST-UBC9, 5 μM SAE1/SAE2 (small scale) or Aos1/Uba2 (large scale), 10 mM ATP, 5 mM $MgCl_2$, 5 mM dithiothreitol, 10 mM NaCl, and 50 mM Tris at pH 7.5 (43). To prepare the ^{15}N-Ets-$1^{(1-138)}$:SUMO-1_{gg} and ^{15}N-Ets-$1^{(1-52)}$:SUMO-1_{gg} complexes, the His_6-tag was initially cleaved off all of the components except SUMO-1_{gg}. For the ^{15}N-SUMO-1_{gg}:Ets-$1^{(1-138)}$ and ^{15}N-SUMO-1_{gg}:Ets-$1^{(1-52)}$ complexes, the His_6-tag was cleaved off all of the components except Ets-$1^{(1-138)}$ or Ets-$1^{(1-52)}$. The desired complexes were isolated by Ni^{2+}-affinity chromatography and purified further with Fractogel-DEAE cation exchange chromatography (Merck) using a 0–750 mM NaCl gradient in 20 mM Tris, 5 mM β-mercaptoethanol, pH 7.5. The resulting ^{15}N-Ets-$1^{(1-138)}$:SUMO-1_{gg} and ^{15}N-Ets-$1^{(1-52)}$:SUMO-1_{gg} were dialyzed into 10 mM KCl, 10 mM potassium phosphate, 5 mM dithiothreitol, 0.1 mM EDTA, pH 6.5, whereas the ^{15}N-SUMO-1_{gg}:Ets-$1^{(1-138)}$ was dialyzed into this buffer plus 100 mM KCl. Thrombin was included during dialysis to remove the His_6-tag, as described above. The final protein complexes were concentrated by ultrafiltration to ~0.5 mM, and D_2O was added to ~10%. Both preparations had an ~33% yield. SDS-PAGE and electrospray ionization mass spectrometry were used to confirm the masses of the complexes.

NMR Spectroscopy—Spectra for UBC9, Ets-$1^{(1-138)}$, and the Ets-$1^{(1-138)}$ derivatives were recorded at 30 °C on a Varian Inova 600 MHz spectrometer. Spectra for SUMO-1_{gg} (17 °C) and for Ets-$1^{(1-52)}$ and its derivatives (22 °C) were recorded on a Varian Unity 500 MHz spectrometer. Samples were in 100 or 10 mM KCl, respectively, with 100 mM potassium phosphate, 5 mM dithiothreitol, 0.1 mM EDTA at pH 6.5. The reduced temperature helped limit protein aggregation and/or degradation. The $^1H^N$, ^{15}N, $^{13}C^\alpha$, and $^{13}C^\beta$ assignments for unmodified $^{13}C/^{15}N$-labeled Ets-$1^{(1-138)}$ and Ets-$1^{(1-52)}$ were obtained using standard triple-resonance NMR experiments in conjunction with the published data for Ets-$1^{(29-138)}$ (38). Assignments for residues 1–97 of SUMO-1_{gg} (47, 48) and UBC9 (49) were based on those reported previously. Amide $^1H^N$ and ^{15}N assignments for ^{15}N-SUMO-1_{gg}, ^{15}N-UBC9, ^{15}N-Ets-$1^{(1-138)}$:SUMO-1_{gg}, ^{15}N-Ets-$1^{(1-52)}$:SUMO-1_{gg}, and ^{15}N-SUMO-1_{gg}:Ets-$1^{(1-138)}$, including those of the isopeptide ^{1}H-$^{15}N^\zeta$ (43), were confirmed using three-dimensional ^{15}N-NOESY- and TOCSY-HSQC spectra. Spectral processing and analysis were carried out using NMRPipe (50) and Sparky (51). Amide ^{15}N relaxation measurements were recorded according to published methods (52).

NMR-monitored titrations of Ets-1 derivatives and UBC9 started with 500 μl of 400 μM labeled protein, to which aliquots of unlabeled protein (1–2 mM) in the same buffer were added in 10 steps to a final molar excess of 4:1. Equilibrium dissociation constants were determined by non-linear least squares fitting of the observed chemical shifts of the labeled protein *versus* the concentration of added unlabeled protein to the equation describing the formation of a 1:1 complex in the fast exchange limit (53). Data are reported based on the average and S.D. for 6–10 amides showing the largest spectral perturbations.

RESULTS

Ets-1 Is Sumoylated in Vivo and in Vitro—Consistent with four consensus sites, full-length Ets-1 was conjugated to SUMO-1 at multiple positions *in vivo*. However, this sumoylation was significantly reduced by the mutation of Lys-15 to an arginine, suggesting that this lysine is the major site of modification (Fig. 1*B*). Importantly, this consensus sequence has been implicated previously in Ets-1 as a "synergy control motif" that mediates transcriptional repression *in vivo* on promoter

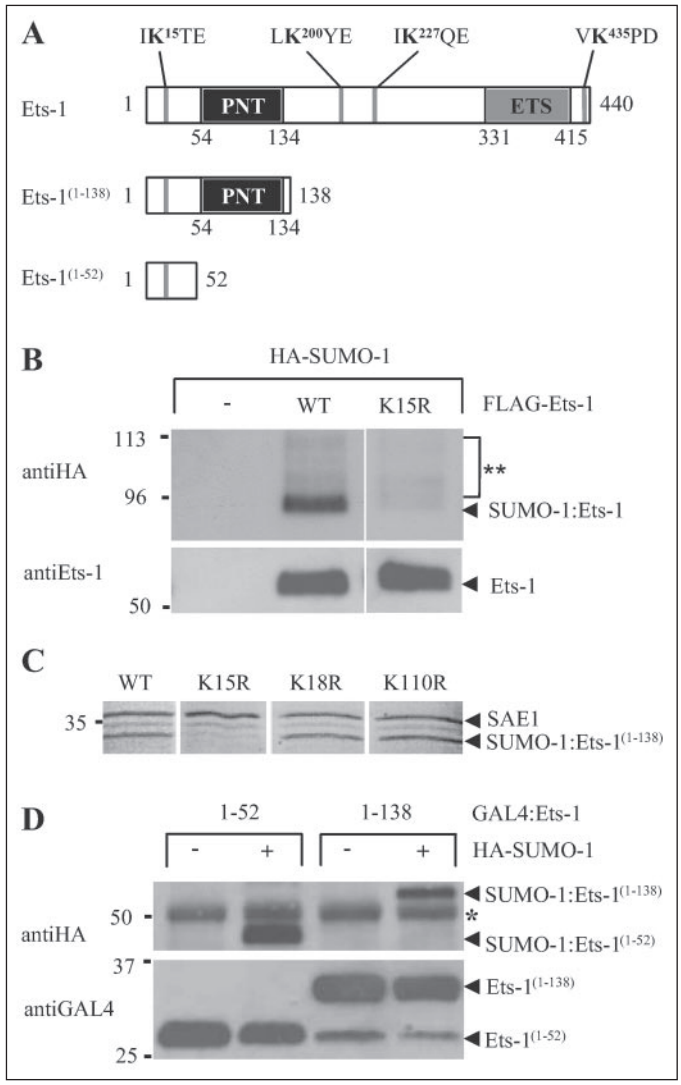

FIGURE 1. **Sumoylation of Ets-1 at Lys-15.** *A*, summary of the domain structure and consensus sumoylation sites in murine Ets-1. The PNT domain (*black*) and DNA-binding ETS domain (*gray*) are indicated (38, 63). *B*, full-length Ets-1 was sumoylated *in vivo*, and mutation of Lys-15 significantly reduced this modification. NIH 3T3 cells were transfected with plasmids expressing HA-tagged SUMO-1 without or with the indicated FLAG-tagged Ets-1 species. Ets-1 was immunoprecipitated using a FLAG antibody followed by immunoblotting with an HA antibody. Ets-1 species were detected in an immunoblot with an Ets-1-specific antibody (*lower panel*). Based on expected molecular masses, single and multiple-sumoylated (**) Ets-1 species are identified. *C*, Ets-$1^{(1-138)}$ was sumoylated *in vitro* at Lys-15 but not Lys-18 or Lys-110. Shown are Coomassie-stained SDS-PAGE gels with the products of *in vitro* reactions using purified sumoylating reagents and the indicated wild type (*WT*) or mutant Ets-$1^{(1-138)}$ species with lysine to arginine point mutations. Only the substitution of Lys-15 with arginine or alanine (not shown) abrogated SUMO-1 conjugation. In addition to its apparent molecular mass, the band corresponding to SUMO-1:Ets-$1^{(1-138)}$ was identified by its absence in control reactions lacking one of ATP, SAE1/SAE2, UBC9, SUMO-1_{gg}, or the Ets-$1^{(1-138)}$ species (not shown). *D*, both Ets-$1^{(1-52)}$ and Ets-$1^{(1-138)}$ were efficiently sumoylated *in vivo*. NIH 3T3 cells were transfected with plasmids expressing GAL4:Ets-$1^{(1-52)}$ or GAL4:Ets-$1^{(1-138)}$ fusion proteins with or without HA-tagged SUMO-1. Ets-1 fusions were immunoprecipitated with GAL4 specific antibodies then probed by immunoblotting with HA-specific antibodies to detect conjugated SUMO-1. Levels of the immunoprecipitated Ets-1 species were detected by subsequent immunoblotting with GAL4-specific antibody; the weak band at the approximate position of GAL4:Ets-$1^{(1-52)}$ in the GAL4:Ets-$1^{(1-138)}$ lanes may result from degradation. In a control experiment, the GAL4 was present at similar levels, but was not sumoylated (data not shown). The * indicates cross-reactivity of anti-rabbit secondary with the heavy chain of mouse α-GAL4, which was conjugated to the immunobeads. Apparent molecular masses (kDa) are marked on all immunoblots.

elements with multiple factor binding sites (54). These motifs are now known to represent sumoylation sites (55). Furthermore, functional data suggest that the sequence containing Lys-15 acts independently, or at least additively with other sites, as mutation of this residue only par-

tially reduces the repression effect (54). Given this independence, we have focused on Lys-15 as the predominant SUMO-1 acceptor lysine in Ets-1. Consistent with these *in vivo* studies, purified Aos1/Uba1 and UBC9 sumoylated Ets-$1^{(1-138)}$ *in vitro* (Fig. 1*C*). Substitution of Lys-15 with an arginine or alanine abrogated this modification. In contrast, mutation of Lys-18 or Lys-110 to arginine did not prevent sumoylation of Ets-$1^{(1-138)}$. The former lysine lies within a pseudo-consensus sequence (EK^{18}VD), whereas the latter is not part of a consensus sequence (GK^{110}EC), yet corresponds to a reported sumoylation site in the PNT domain of human TEL (TK^{99}ED (37)). Thus, Lys-15 is the only target of sumoylation within the N-terminal fragment of Ets-1.

Interaction Surfaces between Ets-$1^{(1-138)}$ and UBC9 Are Mapped by NMR—The non-covalent interaction of Ets-$1^{(1-138)}$ with the E2 SUMO-conjugating enzyme, UBC9, was investigated by NMR spectroscopy. Specifically, ^{1}H-^{15}N HSQC spectra of one ^{15}N-labeled protein were recorded upon titration with a second, unlabeled protein. The chemical shift of an amide group is highly sensitive to changes its local environment resulting from the formation of a protein-protein complex. Mapping chemical shift perturbations onto the structure of the labeled protein provides a qualitative identification of the association interface for its unlabeled partner, and fitting of these titration data to an equilibrium isotherm yields a quantitative measure of their binding affinity (56).

Complementary titrations confirmed that the consensus sumoylation site containing Lys-15 in Ets-$1^{(1-138)}$ binds UBC9 near its active site Cys-93 (Figs. 2 and 3*A*). Upon addition of unlabeled UBC9, selected peaks in the ^{1}H-^{15}N HSQC spectra of ^{15}N-Ets-$1^{(1-138)}$ showed progressive chemical shift changes, indicative of association in the fast exchange limit. When mapped onto the NMR-derived structure of Ets-$1^{(1-138)}$, residues experiencing the largest shift perturbations clustered near Lys-15, the SUMO-1 acceptor site identified by mutational studies. The absence of any significant chemical shift changes for the K15A mutant of ^{15}N-Ets-$1^{(1-138)}$, as well as for ^{15}N-Ets-$1^{(29-138)}$, when titrated with UBC9 confirmed that the binding of these proteins was dependent upon the presence of Lys-15 (Fig. 3, *C* and *D*). Furthermore, these data indicated that the PNT domain did not interact appreciably with UBC9. Indeed, ^{15}N-Ets-$1^{(1-52)}$, which lacks this domain, also bound UBC9 as evident by chemical shift perturbations near Lys-15 similar to those observed with ^{15}N-Ets-$1^{(1-138)}$ (Fig. 3, *A* and *B*). Fitting the titration data recorded for the ^{15}N-labeled Ets-1 fragments yielded a K_d of 420 ± 80 μM for the Ets-$1^{(1-138)}$/UBC9 complex and 800 ± 100 μM for the binding of UBC9 and Ets-$1^{(1-52)}$. Thus, in accord with chemical shift perturbation mapping, the consensus sumoylation site at Lys-15 in the N-terminal region of Ets-1 is the primary determinant for UBC binding. However, the small ~2-fold decrease in the K_d value measured for Ets-$1^{(1-138)}$ may result from a weak or nonspecific contribution of the PNT domain toward complex formation.

NMR titrations were also used to identify the Ets-1 binding interface on the surface of UBC9. Amides in ^{15}N-UBC9 surrounding the active site Cys-93, including the adjacent β-strands S6 (residues 85–88) and S7 (residues 90–92) and helix H3 (residues 131–139), showed chemical shift perturbations when titrated with unlabeled Ets-$1^{(1-138)}$ (Fig. 2) and Ets-$1^{(1-52)}$, but not with Ets-$1^{(51-138)}$ (supplemental Fig. S1). The former two species contain Lys-15, whereas the latter fragment corresponds to the isolated PNT domain. A similar pattern of chemical shift changes was seen in UBC9 upon titration with the C-domain of human RanGAP1 (43), as well as with peptide models of the sumoylation sites from p53 and c-Jun (57). These amides correspond well with the intermolecular interface observed in the crystal complex of mouse RanGAP1 and human UBC9 (12). Thus, the complementary NMR titrations indicate that Ets-1 binds UBC9 such that Lys-15 is positioned near Cys-93, as required for SUMO-1 conjugation.

These NMR measurements also suggest that sumoylation of Lys-15 occurred independently of the remainder of Ets-1, including the PNT domain. To confirm that this *in vitro* phenomenon parallels *in vivo* activity, we tested the *in vivo* sumoylation of Ets-$1^{(1-138)}$ and Ets-$1^{(1-52)}$ in the context of GAL4 fusion proteins. Indeed, both constructs were conjugated with apparent equal efficiency to a tagged version of SUMO-1 (Fig. 1*D*). Thus, the determinants for sumoylation of the N-terminal region of Ets-1 lie within the unstructured N-terminal extension that contains Lys-15.

Ets-1 with Arg-15 Binds UBC9—Although substitution of Lys-15 with Arg eliminated the sumoylation of Ets-$1^{(1-138)}$, the mutant protein still bound UBC9. When ^{15}N-Ets-$1^{(1-138)}$-K15R was titrated with UBC9, chemical shift perturbations similar to those found with the wild type protein were also observed near position 15 (Fig. 3*E*). Fitting of the titration data yielded a K_d of 440 ± 120 μM. Therefore, the side chain guanido group of an arginine residue can substitute for the amino group of a lysine in the binding of Ets-$1^{(1-138)}$ to UBC9.

SUMO-1 and Ets-1 Are Linked by a Flexible Isopeptide Tether—As a step toward understanding how sumoylation alters the biological function of Ets-1, we used NMR spectroscopy to examine the possible structural and dynamic consequences of this post-translational modification. SUMO-1_{gg} and Ets-$1^{(1-138)}$ did not interact non-covalently, as demonstrated by the lack of any selective amide intensity or chemical shift perturbations in the ^{1}H-^{15}N HSQC spectrum of either ^{15}N-labeled protein upon titration with a 4-fold molar excess of the other (data not shown). Upon covalent linkage to SUMO-1_{gg}, the HSQC spectrum of the resulting ^{15}N-Ets-$1^{(1-138)}$:SUMO-1_{gg} complex overlapped closely with that of free ^{15}N-Ets-$1^{(1-138)}$ (Fig. 4*A* and supplemental Fig. S2). With the exception of the appearance of a new signal from the isopeptide ^{1}H-^{15}N$^{\varepsilon}$, the only small spectral changes of note occurred for the chemical shifts of amides near Lys-15, to which SUMO-1_{gg} was attached. The same behavior was observed when ^{15}N-Ets-$1^{(1-52)}$ was modified to yield ^{15}N-Ets-$1^{(1-52)}$:SUMO-1_{gg} (supplemental Fig. S4). Using the complementary labeling approach, the HSQC spectrum of the ^{15}N-SUMO-1_{gg}:Ets-$1^{(1-138)}$ complex was superimposed on that of free ^{15}N-SUMO-1_{gg}. Chemical shift changes occurred only for Gly-96 and Gly-97, as expected because of the conversion of the charged C-terminal carboxylate to a neutral isopeptide (Fig. 4*B* and supplemental Fig. S3). Furthermore, no detectable non-covalent interactions occurred between any regions of the two proteins, including the PNT domain. These data clearly indicated that upon sumoylation the conformations of Ets-$1^{(1-138)}$ and SUMO-1_{gg} were not perturbed beyond the site of their covalent attachment. A similar conclusion was reported for isopeptide-linked complex of SUMO-1_{gg} and the C-terminal domain of RanGAP1 (43).

The dynamic consequences of Ets-1 sumoylation were examined using ^{15}N relaxation studies. These experiments provide a measure of both the global rotational diffusion of a protein, as well as the local mobility of its polypeptide backbone on a residue-specific basis. In particular, the heteronuclear NOE is a sensitive indicator of local dynamics on a ns–ps timescale with values at a ^{15}N frequency of 50.7 MHz decreasing from +0.82 to −3.6 with increasing mobility of a ^{1}H-^{15}N group (58). For example, the well structured PNT domain exhibited high ^{1}H-^{15}N NOE values, whereas the ~50 N-terminal and 4 C-terminal residues in Ets-$1^{(1-138)}$ showed dramatically lower values (Fig. 5*A*) (38). Along with the random-coil amide chemical shifts of these residues, this clearly demonstrated that the consensus sumoylation site at Lys-15 (as well as the ERK2 phosphoacceptor Thr-38) fall within an unstructured and highly mobile region of Ets-1. Not unexpectedly, the entire Ets-$1^{(1-52)}$ had low ^{1}H-^{15}N NOE values, indicative of a random coil-like behavior of this polypeptide (supplemental Fig. S5). Using

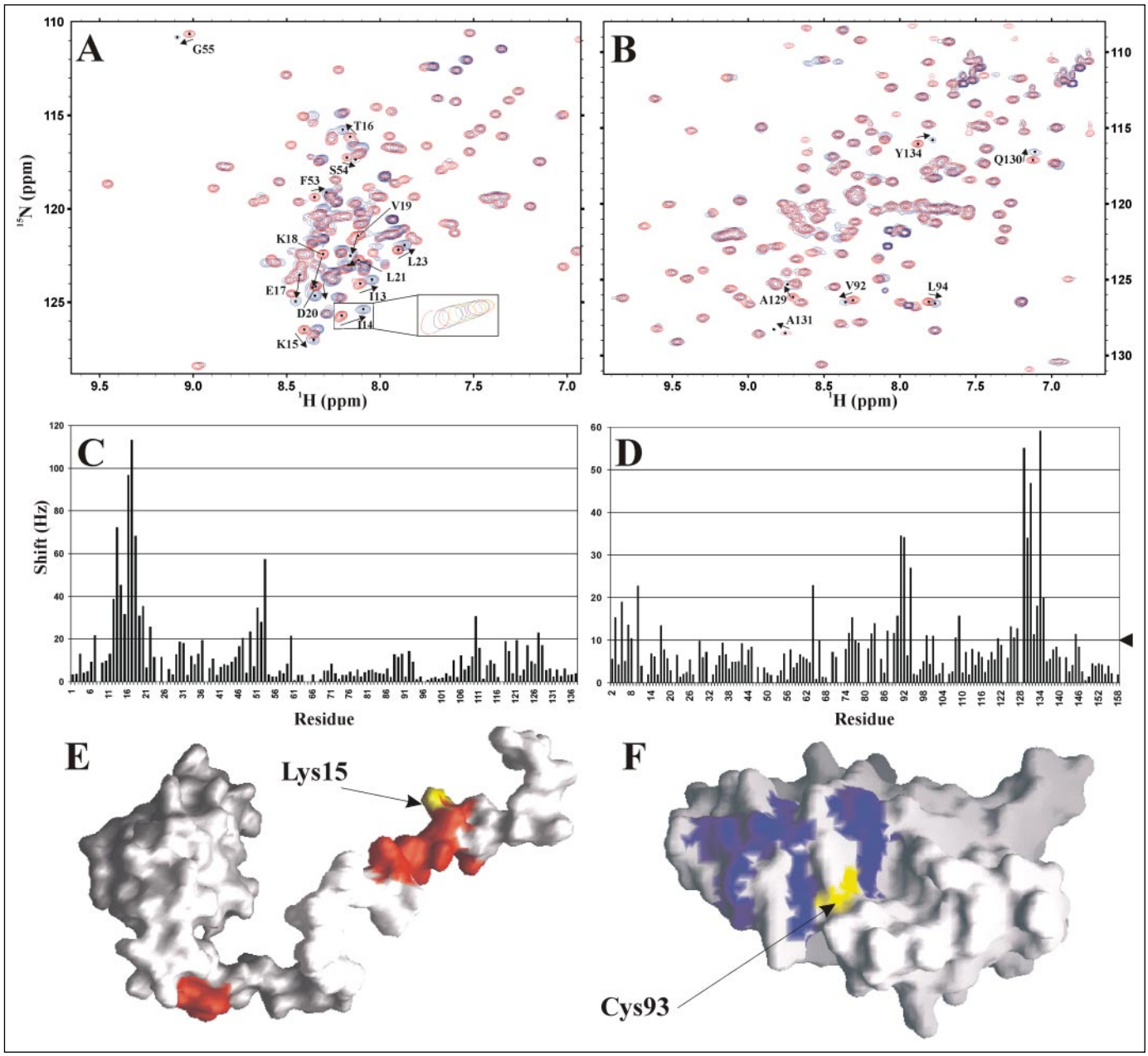

FIGURE 2. **The consensus sumoylation site in the flexible N-terminal region of Ets-1$^{(1-138)}$ binds UBC9 near its active site.** Shown are superimposed ^{1}H-^{15}N HSQC spectra of ^{15}N-Ets-1$^{(1-138)}$ (*A*) and ^{15}N-UBC9 (*B*) in the absence (*red*) and presence (*blue*) of a 4-fold molar excess of unlabeled UBC9 or Ets-1$^{(1-138)}$, respectively (30 °C, pH 6.5). Selected peaks exhibiting shift perturbations because of complex formation are labeled, and the *inset* in *A* illustrates the position of the Ile-14 signal as a function of increasing concentrations of UBC9. The fully annotated spectrum of ^{15}N-Ets-1$^{(1-138)}$ is provided in supplemental Fig. S2 and that of ^{15}N-UBC9 is published (49). The amide chemical shift changes, calculated as $\{(\Delta\omega_H)^2 + (\Delta\omega_N)^2\}^{1/2}$ at 600 MHz, resulting from the addition of a 4-fold molar excess of unlabeled partner, are plotted for ^{15}N-Ets-1$^{(1-138)}$ (*C*) and ^{15}N-UBC9 (*D*). Missing data points correspond to prolines or amino acids with overlapping peaks. Residues that display the largest shift perturbations (above the *arrowhead*) localize spatially near Lys-15 in the consensus sumoylation site of Ets-1$^{(1-138)}$ and Cys-93 in the catalytic site of UBC9, as highlighted in colors on a model of Ets-1$^{(1-138)}$ based on one member of the NMR-derived structural ensemble of Ets-1$^{(29-138)}$ (*E*) (PDB code 1BQV) or the crystallographic structure of UBC9 (*F*) (PDB code 1KPS). The perturbations near Gly-55 at the N-terminal boundary of the Ets-1$^{(1-138)}$ PNT domain may arise because of small changes in sample conditions, as illustrated by control titrations (Fig. 3 and not shown), or a weak interaction with UBC9.

the same approach, we and others (43, 47, 48) have shown that the N- and C-terminal tails of SUMO-1$_{gg}$, including Gly-96 and Gly-97, are also highly flexible. Upon sumoylation, the NOE relaxation profile of Ets-1$^{(1-138)}$ (Fig. 5*B*) and Ets-1$^{(1-52)}$ (supplemental Fig. S5) did not change except for residues near Lys-15. The localized increase in the ^{1}H-^{15}N NOE values for these residues is expected because of the presence of the covalently attached SUMO-1$_{gg}$. Nevertheless, these low NOE values (<0.4) indicated that, even when sumoylated, the N-terminal region of Ets-1 is conformationally mobile. This is consistent with the lack of any induced structure within this region, as evidenced by the absence of any significant spectral perturbations. Furthermore, the isopeptide ^{15}N$^{\zeta}$ had an NOE value of ~0.0 verifying that the side chain of Lys-15 is also very mobile when linked to Gly-97 of SUMO-1$_{gg}$.

DISCUSSION

Ets-1 Is Sumoylated at Lys-15 within Its Unstructured N-terminal Sequence—To investigate the structural principles of SUMO addition to substrates, we exploited a well characterized deletion fragment, Ets-1$^{(1-138)}$ that bears a single site of sumoylation. *In vitro* and *in vivo* assays of wild type and mutant forms of this fragment con-

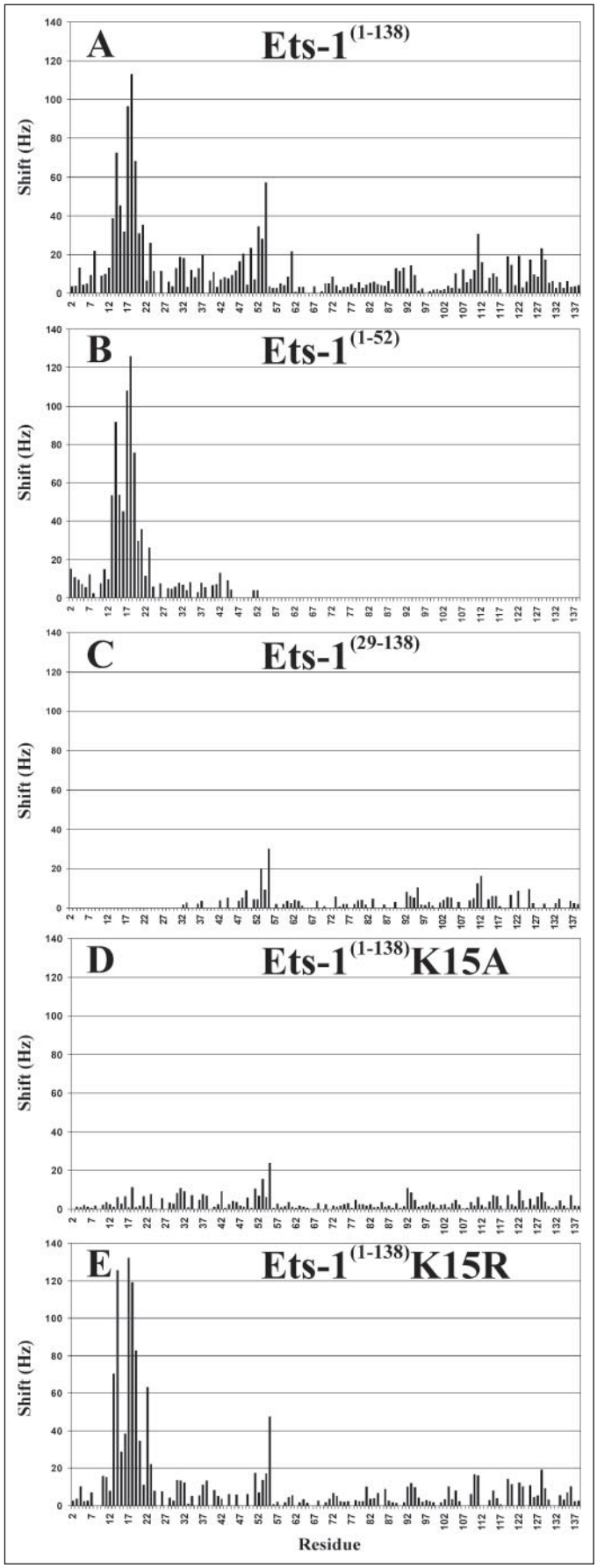

firmed that Lys-15 is the acceptor for SUMO-1 attachment. In parallel, NMR spectroscopic studies demonstrated chemical shift perturbations only for amides flanking Lys-15 when ^{15}N-Ets-1$^{(1-138)}$ was titrated with unlabeled UBC9. Complementary measurements with ^{15}N-UBC9 revealed that the chemical shifts of amides adjacent to Cys-93 changed upon addition of Ets-1$^{(1-138)}$. Thus, the binding of Ets-1$^{(1-138)}$ to UBC9 likely positions Lys-15 in close proximity to Cys-93, allowing direct sumoylation by the conjugating enzyme. Although not required, the efficiency of this reaction could be increased *in vivo* by a yet unidentified SUMO E3-ligase.

The N-terminal segment of Ets-1 containing Lys-15 is unstructured in solution, as evidenced by random coil NMR chemical shifts (38) and low heteronuclear ^{1}H-^{15}N NOE values. The dynamic properties of this accessible sequence may facilitate its binding in an extended conformation to the shallow active site groove of UBC9 (12, 43, 57). Such conformational flexibility appears to be a general feature of many proteins that are post-translationally modified with SUMO. Similar to Ets-1, characterized sumoylation sites frequently occur within the unstructured N- or C-terminal tails of proteins or in linker regions between structured domains. This may allow for more efficient access of the target lysine to the sumoylation/desumoylation machinery, as well as provide flexibility for SUMO-dependent interactions with one or more downstream effectors. However, exceptions occur (2, 7, 8), as evidenced by the reported sumoylation of TEL at a lysine within an α-helix in its structured PNT domain (23, 37). Ets-1 is not modified at the homologous Lys-110 in its PNT domain. Interestingly, similar to Ets-1$^{(1-138)}$, murine Tel$^{(1-126)}$ with the mutation A94D that disrupts its self-association (59) is sumoylated *in vitro* at a consensus site (IK^{11}QE) within its unstructured N-terminal segment, but not within its PNT domain.[6] Human TEL, with this mutation, is also reported to no longer undergo sumoylation *in vivo* (23). Thus, the conjugation of SUMO to the PNT domain of TEL may require its polymerization and may be facilitated *in vivo* by an E3 ligating enzyme.

Based on NMR titration data, the K_d value for the dissociation of the Ets-1$^{(1-138)}$ complex with UBC9 is ~400 μM. This value is 800-fold weaker than that of ~0.5 μM reported for the binding of the C-terminal domain of human RanGAP1 with UBC9 (60) and ~10-fold stronger that those of ~3–6 mM measured for peptide models of sumoylation sites from p53 and c-Jun (57). The differences in these affinities may in part reflect the exact sequences flanking the SUMO acceptor lysine in each protein. However, the significantly tighter binding of RanGAP1 to UBC9, which correlates with its unusually high level of sumoylation *in vivo*, could arise from two additional factors. First, the SUMO acceptor site in RanGAP1 is located in an exposed loop between helices H6 and H7 of its C-terminal domain (12). Although this loop is conformationally flexible relative to the core helices in RanGAP1, ^{1}H-^{15}N NOE relaxation measurements indicate that it is significantly less dynamic than the unstructured N-terminal region of Ets-1 (43). Thus the sumoylation site of RanGAP1 may be partially constrained in an extended conformation suited for binding the shallow active site groove of UBC9. This

[6] M. S. Macauley, W. J. Errington, M. Schärpf, C. D. Mackereth, and L. P. McIntosh, unpublished observations.

FIGURE 3. **Ets-1 fragments containing Lys-15 or Arg-15 bind UBC9.** Shown are amide chemical shifts changes, calculated as $\{(\Delta\omega_H)^2 + (\Delta\omega_N)^2\}^{1/2}$ at 600 MHz, for ^{15}N-labeled Ets-1$^{(1-138)}$ (*A*), Ets-1$^{(1-52)}$ (*B*), Ets-1$^{(29-138)}$ (*C*), Ets-1$^{(1-138)}$-K15A (*D*), and Ets-1$^{(1-138)}$-K15R (*E*) (400 μM starting concentration) resulting from the addition of a 4-fold molar excess of UBC9 at 30 °C, pH 6.5. *A* is reproduced from Fig. 2*C* for direct comparison. Ets-1 fragments containing Lys-15 or Arg-15 bind UBC9, as evidenced by chemical shift perturbations for amides near this position, whereas those with Ala-15 or with residues 1–28 deleted do not bind.

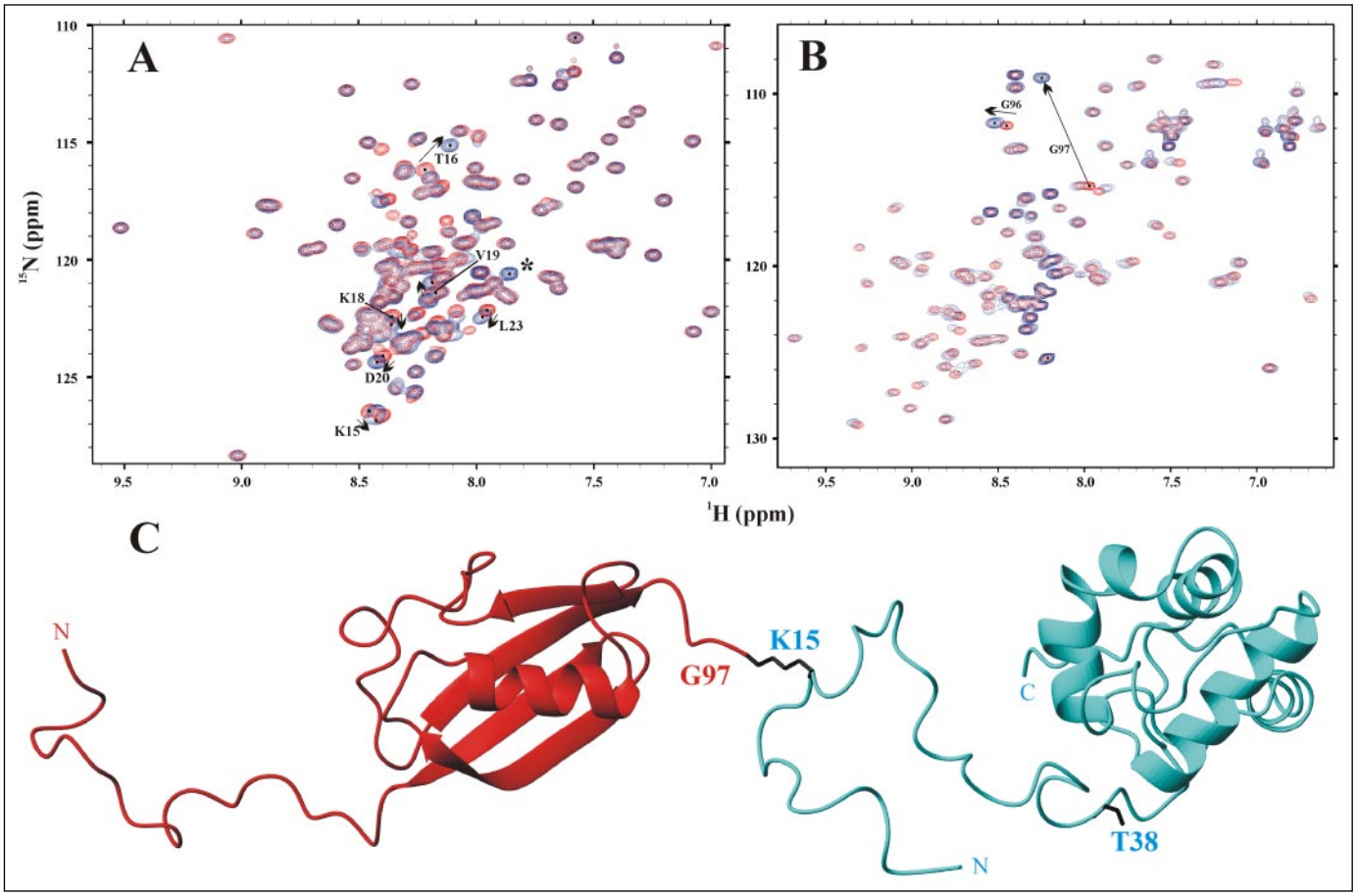

FIGURE 4. **Structures of Ets-1$^{(1-138)}$ and SUMO-1$_{gg}$ are not altered beyond the site of sumoylation.** With the exception of residues immediately adjacent to the isopeptide bond, there were no spectral, and hence structural, perturbations in either protein because of their covalent attachment. *A*, overlaid ^{1}H-^{15}N HSQC spectra of ^{15}N-Ets-1$^{(1-138)}$ (*red*) and ^{15}N-Ets-1$^{(1-138)}$:SUMO-1$_{gg}$ (*blue*) at pH 6.5 and 30 °C. Peaks from amides near Lys-15 are labeled. The * indicates the signal from the ^{1}H-^{15}N$^{\varepsilon}$ of the new isopeptide between Lys-15 of Ets-1$^{(1-138)}$ and Gly-97 of SUMO-1$_{gg}$, assigned on the basis of interproton NOESY interactions between these two residues (not shown). *B*, overlaid ^{1}H-^{15}N HSQC spectra of ^{15}N-SUMO-1$_{gg}$ (*red*) and ^{15}N-SUMO-1$_{gg}$:Ets-1$^{(1-138)}$ (*blue*) at pH 6.5 and 17 °C. The *arrows* indicated the changes in the chemical shifts of Gly-96 and Gly-97 resulting from covalent bonding to Lys-15. Note that only signals from the ^{15}N-labeled member of the protein complexes are detected in these spectra. Minor changes in chemical shifts or peak intensities are attributed to small differences in pH or ionic strength between the protein samples as demonstrated by control measurements (not shown). Fully annotated spectra are provided in supplemental Fig. S2 and S3. *C*, beads-on-a-string model of Ets-1$^{(1-138)}$:SUMO-1$_{gg}$ in which Lys-15, within the unstructured N-terminal segment of Ets-1$^{(1-138)}$ (*cyan*), is covalently linked to the flexible C-terminal Gly-97 of SUMO-1$_{gg}$ (*red*). Neither the structure nor dynamic properties of the two proteins are perturbed beyond the site of their covalent linkage, and the isopeptide is conformationally mobile on the subnanosecond timescale. Because of this flexibility, the model (based on PDB codes 1BQV and 1A5R) is only a snapshot of a large ensemble of possible orientations for the two proteins.

would lead to a lower entropic penalty for association with UBC9 than incurred by the unconstrained target sites in Ets-1$^{(1-138)}$ or the peptide models of p53 and c-Jun. Second, in addition to intermolecular contacts between the consensus sumoylation sequence of RanGAP1 and the active site region of UBC9 near Cys-93, interactions are also observed with residues in helices H6 and H7 of RanGAP1 and helix H3 of UBC9 (12). This discontinuous binding interface would not be present with sumoylation sites in unstructured linear sequences of target proteins such as Ets-1.

Sumoylation Sites with Lysine to Arginine Substitutions Bind UBC9—Substitution of Lys-15 with arginine abrogates the sumoylation of Ets-1$^{(1-138)}$. However, NMR-monitored titrations demonstrate that Ets-1$^{(1-138)}$ containing Arg-15 binds with similar affinity to the same active site region of UBC9 as does the wild type species. In the crystal structure of the RanGAP1/UBC9 complex, the amino group of the RanGAP1 SUMO acceptor Lys-526 is hydrogen-bonded to the side chain carboxyl of Asp-127 of UBC9 and to an ordered water molecule, while also lying in close proximity to the S$^{\gamma}$ of Cys-93 (12). It is reasonable that an arginine can mimic these interactions. Because of this mimicry, a ψ*RXE*/D sequence will act as a competitive inhibitor of a consensus sumoylation site for binding to UBC9. This may provide an avenue for disrupting sumoylation *in vivo*.

Covalently Linked Ets-1 and SUMO-1 Are Beads-on-a-String—Isopeptide-linked Ets-1$^{(1-138)}$ and SUMO-1$_{gg}$ are beads-on-a-string with no significant structural interactions between the two proteins beyond the site of their covalent attachment (Fig. 4*C*). Evidence for this behavior derives from both structural and dynamic NMR spectroscopic studies of the purified Ets-1$^{(1-138)}$:SUMO-1$_{gg}$ complex. The ^{1}H-^{15}N HSQC spectrum of each selectively labeled protein in the complex resembles closely that of its isolated form, with chemical shift changes localized to the C-terminal Gly-96 and Gly-97 of SUMO-1$_{gg}$ and to amides near Lys-15 in Ets-1$^{(1-138)}$. Thus, no detectable structural perturbations occur in either protein beyond the site of their linkage via the Lys-15–Gly-97 isopeptide bond. This includes the absence of any induced structure within the N-terminal region of Ets-1$^{(1-138)}$ and a lack of any non-covalent interactions between the PNT domain and SUMO-1$_{gg}$. Furthermore, ^{15}N relaxation measurements reveal that the unstructured N-terminal region of Ets-1$^{(1-138)}$ remains conformationally mobile on a ns–ps timescale upon sumoylation, albeit with somewhat dampened mobility near Lys-15 because of excluded volume effects

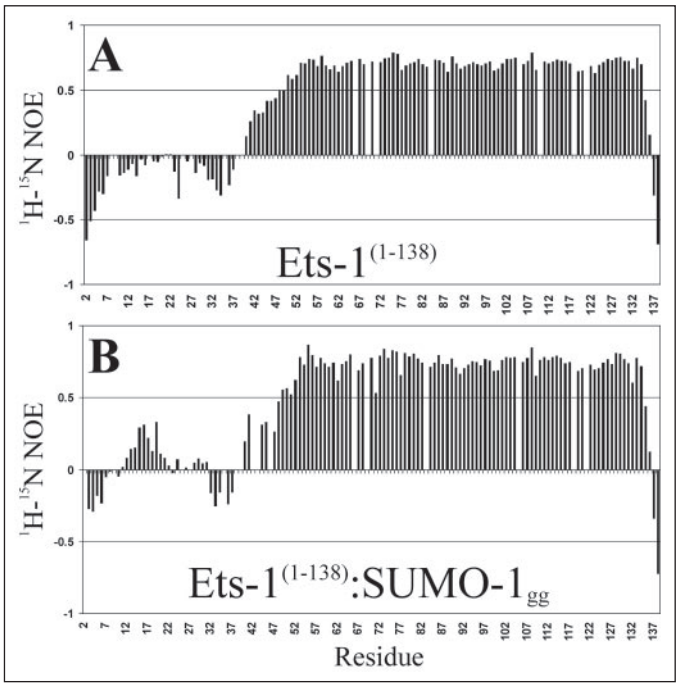

FIGURE 5. **Dynamics of Ets-1$^{(1-138)}$ are not affected beyond the site of sumoylation.** Except for residues adjacent to the isopeptide bond at Lys-15, there were no changes in the fast timescale backbone motions of Ets-1$^{(1-138)}$ upon covalent attachment of SUMO-1$_{gg}$. Shown are the steady-state ^{1}H-^{15}N NOE values of ^{15}N-Ets-1$^{(1-138)}$ (*A*) and ^{15}N-Ets-1$^{(1-138)}$:SUMO-1$_{gg}$ (*B*) at pH 6.5 and 30 °C (600 MHz). Increasing amide mobility on the ns–ps timescale results in decreasing ^{1}H-^{15}N NOE values. *A*, the folded PNT domain of Ets-1$^{(1-138)}$ is well ordered, whereas the consensus sequence containing Lys-15 lies within its flexible, unstructured N-terminal region. *B*, upon sumoylation, the backbone dynamics of ^{15}N-Ets-1$^{(1-138)}$:SUMO-1$_{gg}$ were only dampened partially near Lys-15. The isopeptide ^{15}N$^{\zeta}$ had a NOE value of −0.11 (not shown), indicating that it is also very mobile. Missing data points corresponded to prolines or residues with severe spectral overlap. Errors are ~5%.

and/or hydrodynamic drag from the covalently linked SUMO-1$_{gg}$. With a ^{1}H-^{15}N NOE value of ~0 for its isopeptide ^{15}N$^{\zeta}$, the side chain of Lys-15 is also highly mobile on this timescale when bonded to Gly-97 of SUMO-1$_{gg}$. Similar results were observed for the covalent complex of SUMO-1$_{gg}$ with Ets-1$^{(1-52)}$, a deletion fragment containing only the unstructured N-terminal sequence of Ets-1.

Recently, three SUMO conjugates have been characterized structurally. Similar to Ets-1$^{(1-138)}$:SUMO-1$_{gg}$, NMR spectroscopic studies demonstrated that the C-terminal domain of RanGAP1 and SUMO-1$_{gg}$ are linked by a flexible isopeptide tether and thus remain structurally and dynamically independent when conjugated (43). The lack of any non-covalent interactions between RanGAP1 and SUMO-1 is also seen in the crystallized complex of isopeptide-linked SUMO-1$_{gg}$:RanGAP1 with UBC9 and a fragment of the E3-ligase RanBP2/Nup358 (6). In contrast, the crystal structure of SUMO-1 with the ubiquitin-conjugating enzyme E2-25K revealed a small but well defined interface between these two proteins at the site of their isopeptide linkage. The isopeptide is also ordered, with a kink occurring in the backbone of SUMO-1 at its C-terminal Gly-97 (8). However, beyond this interface, the structures of E2-25K and SUMO-1 are not perturbed. Interestingly, the non-consensus SUMO-acceptor Lys-14 is located within the basic N-terminal α-helix of E2-25K, indicating that a novel structure-dependent interaction with UBC9 may be required for sumoylation at this site. More dramatically, the crystallographic analysis of thymine DNA glycosylase conjugated to SUMO-1 highlighted two important structural features (7). First, thymine DNA glycosylase and SUMO-1 interact non-covalently with a β-strand from the glycosylase (corresponding to a SUMO-binding motif (61)) pairing to the β-sheet of SUMO-1. Second, sumoylation appears to induce formation of an α-helix in thymine DNA glycosylase immediately preceding its isopeptide-linked lysine residue. In contrast to thymine DNA glycosylase, Ets-1$^{(1-138)}$ does not contain a SUMO-binding motif, and its sumoylation does not lead to any induced structure.

Based on these structural studies, several general, non-exclusive models can be envisioned for how SUMO-dependent interactions of a target protein with other macromolecules can impart a cellular response (2). Upon their covalent linkage, the conformation of the target protein and/or SUMO may become altered, thereby sequestering or exposing a new recognition surface on one member of the pair. The model is exemplified by thymine DNA glycosylase, whereby the α-helix allosterically induced upon sumoylation is proposed to promote dissociation of the glycosylase from its product complex with DNA (7). Alternatively, both SUMO and the target protein may largely retain their independent conformations within the context of an isopeptide-linked heterodimer. As with IκBα, SUMO could simply prevent modifications, such as ubiquitinylation or acetylation, of an acceptor lysine residue (62). Sumoylation could also block the association of a target protein with another partner macromolecule. This is exemplified by E2-25K for which SUMO attachment appears to interfere with its interaction with the ubiquitin E1-activating enzyme, thereby impairing ubiquitin thioester bond formation (8). Conversely, SUMO could act as a tag or docking module, bridging the isopeptide-linked protein to a second SUMO-binding protein. However, in the case where a macromolecule specifically recognizes the sumoylated protein, but not SUMO or the unmodified protein alone, it is likely that both SUMO and the modified protein co-operatively contribute determinants to a new multipartite binding interface for that macromolecule or macromolecular complex. The isopeptide may also be present in this interface. Given the beads-on-a-string behavior of Ets-1$^{(1-138)}$:SUMO-1$_{gg}$, it is likely that the biological consequences of Ets-1 sumoylation arise through these latter mechanisms, rather than any induced conformational changes. Furthermore, the flexibility of the polypeptide segment linking Ets-1 and SUMO-1 may translate into plasticity important for the binding of one or more signaling or transcriptional regulatory macromolecules. Indeed, based on our NMR studies of sumoylated Ets-1$^{(1-138)}$ and RanGAP1 (43), we hypothesize that such flexibility may be a general feature contributing to the recognition of SUMO- and other ubiquitin-like protein-modified proteins by their downstream effectors.

In summary, we have characterized the sumoylation of Ets-1 at the SUMO-acceptor site, Lys-15, within its unstructured N-terminal sequence. This consensus site binds to UBC9 near its catalytic Cys-93, thereby allowing the direct transfer of SUMO from this E2-conjugating enzyme. The covalent attachment of SUMO-1$_{gg}$ to Ets-1$^{(1-138)}$ or Ets-1$^{(1-52)}$ does not perturb the structure or dynamic properties of either protein, indicating that they are beads-on-a-string tethered by a flexible isopeptide linkage. These results provide a framework for understanding the molecular mechanisms by which sumoylation affects Ets-1 activity *in vivo*.

Acknowledgments—We thank Eric Escobar Cabrera and Mark Okon for technical assistance.

REFERENCES

1. Muller, S., Ledl, A., and Schmidt, D. (2004) *Oncogene* **23,** 1998–2008
2. Johnson, E. S. (2004) *Annu. Rev. Biochem.* **73,** 355–382
3. Dohmen, R. J. (2004) *Biochim. Biophys. Acta* **1695,** 113–131
4. Hilgarth, R. S., Murphy, L. A., Skaggs, H. S., Wilkerson, D. C., Xing, H. Y., and Sarge, K. D. (2004) *J. Biol. Chem.* **279,** 53899–53902
5. Hay, R. T. (2005) *Mol. Cell* **18,** 1–12

6. Reverter, D., and Lima, C. D. (2005) *Nature* **435,** 687–692
7. Baba, D., Maita, N., Jee, J. G., Uchimura, Y., Saitoh, H., Sugasawa, K., Hanaoka, F., Tochio, H., Hiroaki, H., and Shirakawa, M. (2005) *Nature* **435,** 979–982
8. Pichler, A., Knipscheer, P., Oberhofer, E., van Dijk, W. J., Korner, R., Olsen, J. V., Jentsch, S., Melchior, F., and Sixma, T. K. (2005) *Nature Struct. Mol. Biol.* **12,** 264–269
9. Gocke, C. B., Yu, H., and Kang, J. (2005) *J. Biol. Chem.* **280,** 5004–5012
10. Rodriguez, M. S., Dargemont, C., and Hay, R. T. (2001) *J. Biol. Chem.* **276,** 12654–12659
11. Matunis, M. J., Wu, J., and Blobel, G. (1998) *J. Cell Biol.* **140,** 499–509
12. Bernier-Villamor, V., Sampson, D. A., Matunis, M. J., and Lima, C. D. (2002) *Cell* **108,** 345–356
13. Mossessova, E., and Lima, C. D. (2000) *Mol. Cell* **5,** 865–876
14. Melchior, F., Schergaut, M., and Pichler, A. (2003) *Trends Biochem. Sci.* **28,** 612–618
15. Wykoff, D. D., and O'Shea, E. K. (2005) *Mol. Cell. Proteomics* **4,** 73–83
16. Wohlschlegel, J. A., Johnson, E. S., Reed, S. I., and Yates, J. R. (2004) *J. Biol. Chem.* **279,** 45662–45668
17. Hannich, J. T., Lewis, A., Kroetz, M. B., Li, S. J., Heide, H., Emili, A., and Hochstrasser, M. (2005) *J. Biol. Chem.* **280,** 4102–4110
18. Verger, A., Perdomo, J., and Crossley, M. (2003) *EMBO Rep.* **4,** 137–142
19. Girdwood, D. W. H., Tatham, M. H., and Hay, R. T. (2004) *Semin. Cell. Dev. Biol.* **15,** 201–210
20. Gill, G. (2005) *Curr. Opin. Genet. Dev.* **15,** 1–6
21. Lin, X., Liang, M., Liang, Y. Y., Brunicardi, F. C., and Feng, X. H. (2003) *J. Biol. Chem.* **278,** 31043–31048
22. Salinas, S., Briancon-Marjollet, A., Bossis, G., Lopez, M. A., Piechaczyk, M., Jariel-Encontre, I., Debant, A., and Hipskind, R. A. (2004) *J. Cell Biol.* **165,** 767–773
23. Wood, L. D., Irvin, B. J., Nucifora, G., Luce, K. S., and Hiebert, S. W. (2003) *Proc. Natl. Acad. Sci. U. S. A.* **100,** 3257–3262
24. Borden, K. L. (2002) *Mol. Cell. Biol.* **22,** 5259–5269
25. Eskiw, C. H., and Bazett-Jones, D. P. (2002) *Biochem. Cell Biol.* **80,** 301–310
26. Girdwood, D., Bumpass, D., Vaughan, O. A., Thain, A., Anderson, L. A., Snowden, A. W., Garcia-Wilson, E., Perkins, N. D., and Hay, R. T. (2003) *Mol. Cell* **11,** 1043–1054
27. Yang, S. H., and Sharrocks, A. D. (2004) *Mol. Cell* **13,** 611–617
28. Chang, C. C., Lin, D. Y., Fang, H. I., Chen, R. H., and Shih, H. M. (2005) *J. Biol. Chem.* **280,** 10164–10173
29. Hong, Y., Rogers, R., Matunis, M. J., Mayhew, C. N., Goodson, M., Park-Sarge, O. K., and Sarge, K. D. (2001) *J. Biol. Chem.* **276,** 40263–40267
30. Yang, S. H., Jaffray, E., Hay, R. T., and Sharrocks, A. D. (2003) *Mol. Cell* **12,** 63–74
31. Bossis, G., Malnou, C. E., Farras, R., Andermarcher, E., Hipskind, R., Rodriguez, M. S., Schmidt, D., Muller, S., Jariel-Encontre, I., and Piechaczyk, M. (2005) *Mol. Biol. Cell* **25,** 6964–6979
32. Hahn, S. L., Criqui, P., and Wasylyk, B. (1997) *Oncogene* **15,** 1489–1495
33. Chakrabarti, S. R., Sood, R., Ganguly, S., Bohlander, S., Shen, Z. Y., and Nucifora, G. (1999) *Proc. Natl. Acad. Sci. U. S. A.* **96,** 7467–7472
34. Leight, E. R., Glossip, D., and Kornfeld, K. (2005) *Development* (*Camb.*) **132,** 1047–1056
35. Wasylyk, C., Criqui-Filipe, P., and Wasylyk, B. (2005) *Oncogene* **24,** 820–828
36. Degerny, C., Monte, D., Beaudoin, C., Jaffray, E., Portois, L., Hay, R. T., de Launoit, Y., and Baert, J. L. (2005) *J. Biol. Chem.* **280,** 24330–24338
37. Chakrabarti, S. R., Sood, R., Nandi, S., and Nucifora, G. (2000) *Proc. Natl. Acad. Sci. U. S. A.* **97,** 13281–13285
38. Slupsky, C. M., Gentile, L. N., Donaldson, L. W., Mackereth, C. D., Seidel, J. J., Graves, B. J., and McIntosh, L. P. (1998) *Proc. Natl. Acad. Sci. U. S. A.* **95,** 12129–12134
39. Seidel, J. J., and Graves, B. J. (2002) *Genes Dev.* **16,** 127–137
40. Foulds, C. E., Nelson, M. L., Blaszczak, A. G., and Graves, B. J. (2004) *Mol. Cell. Biol.* **24,** 10954–10964
41. Cowley, D. O., and Graves, B. J. (2000) *Genes Dev.* **14,** 366–376
42. Bencsath, K. P., Podgorski, M. S., Pagala, V. R., Slaughter, C. A., and Schulman, B. A. (2002) *J. Biol. Chem.* **277,** 47938–47945
43. Macauley, M. S., Errington, W. J., Okon, M., Scharpf, M., Mackereth, C. D., Schulman, B. A., and McIntosh, L. P. (2004) *J. Biol. Chem.* **279,** 49131–49137
44. Best, J. L., Ganiatsas, S., Agarwal, S., Changou, A., Salomoni, P., Shirihai, O., Meluh, P. B., Pandolfi, P. P., and Zon, L. I. (2002) *Mol. Cell* **10,** 843–855
45. Gasteiger, E., Gattiker, A., Hoogland, C., Ivanyi, I., Appel, R. D., and Bairoch, A. (2003) *Nucleic Acids Res.* **31,** 3784–3788
46. Gunther, C. V., and Graves, B. J. (1994) *Mol. Cell. Biol.* **14,** 7569–7580
47. Bayer, P., Arndt, A., Metzger, S., Mahajan, R., Melchior, F., Jaenicke, R., and Becker, J. (1998) *J. Mol. Biol.* **280,** 275–286
48. Jin, C. W., Shiyanova, T., Shen, Z. Y., and Liao, X. B. (2001) *Int. J. Biol. Macromol.* **28,** 227–234
49. Liu, Q., Jin, C. W., Liao, X. B., Shen, Z. Y., Chen, D. J., and Chen, Y. (1999) *J. Biol. Chem.* **274,** 16979–16987
50. Delaglio, F., Grzesiek, S., Vuister, G. W., Zhu, G., Pfeifer, J., and Bax, A. (1995) *J. Biomol. NMR* **6,** 277–293
51. Goddard, T. D., and Kneeler, D. G. (1999) *Sparky 3*, University of California, San Francisco, CA
52. Farrow, N. A., Muhandiram, R., Singer, A. U., Pascal, S. M., Kay, C. M., Gish, G., Shoelson, S. E., Pawson, T., Formankay, J. D., and Kay, L. E. (1994) *Biochemistry* **33,** 5984–6003
53. Johnson, P. E., Tomme, P., Joshi, M. D., and McIntosh, L. P. (1996) *Biochemistry* **35,** 13895–13906
54. Iniguez-Lluhi, J. A., and Pearce, D. (2000) *Mol. Cell. Biol.* **20,** 6040–6050
55. Subramanian, L., Benson, M. D., and Iniguez-Lluhi, J. A. (2003) *J. Biol. Chem.* **278,** 9134–9141
56. Zuiderweg, E. R. P. (2002) *Biochemistry* **41,** 1–7
57. Lin, D., Tatham, M. H., Yu, B., Kim, S., Hay, R. T., and Chen, Y. (2002) *J. Biol. Chem.* **277,** 21740–21748
58. Kay, L. E., Torchia, D. A., and Bax, A. (1989) *Biochemistry* **28,** 8972–8979
59. Kim, C. A., Phillips, M. A., Kim, W., Gingery, M., Tran, H. H., Robinson, M. A., Faham, S., and Bowie, J. U. (2001) *EMBO J.* **20,** 4173–4182
60. Tatham, M. H., Kim, S., Yu, B., Jaffray, E., Song, J., Zheng, J., Rodriguez, M. S., Hay, R. T., and Chen, Y. (2003) *Biochemistry* **42,** 9959–9969
61. Song, J., Durrin, L. K., Wilkinson, T. A., Krontiris, T. G., and Chen, Y. (2004) *Proc. Natl. Acad. Sci. U. S. A.* **101,** 14373–14378
62. Desterro, J. M., Rodriguez, M. S., and Hay, R. T. (1998) *Mol. Cell* **2,** 233–239
63. Lee, G. M., Donaldson, L. W., Pufall, M. A., Kang, H. S., Pot, I., Graves, B. J., and McIntosh, L. P. (2005) *J. Biol. Chem.* **280,** 7088–7099